Hole Detection in Metabolic Connectivity of Alzheimer's Disease Using $k-$Laplacian

Hyekyoung Lee[1], Moo K. Chung[2], Hyejin Kang[1], and Dong Soo Lee[1]

[1] Dept. of Nuclear Medicine, Seoul National University, Republic of Korea
[2] Depart. of Biostatistics and Medical Informatics, University of Wisconsin, Madison, USA
hklee.brain@gmail.com, mkchung@wisc.edu, {hkang211,dsl}@snu.ac.kr

Abstract. Recent studies have found that the modular structure of functional brain network is disrupted during the progress of Alzheimer's disease. The modular structure of network is the most basic topological invariant in determining the shape of network in the view of algebraic topology. In this study, we propose a new method to find another higher order topological invariant, hole, based on persistent homology. If a hole exists in the network, the information can be inefficiently delivered between regions. If we can localize the hole in the network, we can infer the reason of network inefficiency. We propose to detect the persistent hole using the spectrum of $k-$Laplacian, which is the generalized version of graph Laplacian. The method is applied to the metabolic network based on FDG-PET data of Alzheimer disease (AD), mild cognitive impairment (MCI) and normal control (NC) groups. The experiments show that the persistence of hole can be used as a biological marker of disease progression to AD. The localized hole may help understand the brain network abnormality in AD, revealing that the limbic-temporo-parietal association regions disturb direct connections between other regions.

1 Introduction

The hierarchical modular structure of brain network has revealed the functional integration of local specialized modules of brain regions [1]. The modular structure of network is the first basic topological invariant in determining the shape of network in the view of algebraic topology [2]. The second basic topological invariant is holes. While the connected network structures of brain has been often studied, holes never played any role in modeling brain networks [3,1]. However, hole detection has found its usefulness in mobile sensor networks in determining the obstacle-regions, which weaken the strength of cellphone signals [4,5]. In this study, we take a novel hole detection method in finding such aberrant regions of brain network in Alzheimer's disease (AD).

If the brain network has the hole, it implies that the information can be inefficiently transferred between regions due to indirect connections around the hole. When abnormal brain regions associated with Alzheimer's disease interrupt direct connections between other regions, the hole can occur in the network. The

P. Golland et al. (Eds.): MICCAI 2014, Part III, LNCS 8675, pp. 297–304, 2014.

larger the hole is, the more inefficient the information transfer around the hole is. Hence, the size of hole can be a new measure for quantifying the degree of abnormality of the brain network in AD [6]. To find holes and estimate their size, we introduce the concept of persistent homology which assumes that true topological invariants of the underlying network are more persistent over the change of network parameters rather than noise. The more persistent hole is over the change of network parameters, the more connections are needed to cover the hole. Thus, the persistence of hole can be considered as its size. The hole is usually identified by manipulating a matrix associated with the boundary operator in the persistent homology [7]. This method directly selects the edge set that forms a hole. However, this approach has an ambiguity in choosing edges that depends on the order of nodes and edges. A superior new method, which this paper is proposing, is to estimate holes by computing the eigenvectors with zero eigenvalues of higher order Laplacians [5], called k-Laplacian. The method represents the hole as a linear combination of edges of which coefficients are proportional to their contributions to the hole.

The methodological contributions of this paper are: (1) We propose a new method in detecting the local abnormality of network by identifying a hole within the persistent homology framework. This is the first study of using the hole as a brain network feature. (2) We introduce the concept of $k-$Laplacian in estimating the hole. This approach is a natural generalization of finding modular structure of brain network using the spectrum of graph Laplacian, i.e., $0-$Laplacian. (3) We demonstrate that the persistence of holes in the network can be used to quantify the disease progression for the first time. The proposed hole detection method is applied to the FDG-PET based metabolic network of AD, mild cognitive impairment (MCI) and normal control (NC) groups. Our finding suggests that the persistence of hole may be increased as the disease progressed. The resulting holes support prior studies that reported alterations and disconnections in temporal, parietal, frontal association areas and abnormal change in the limbic region by AD [8,9]. In addition, the result also show that the medial temporal lobe is affected by MCI [9].

2 Methods

2.1 $k-$Dimensional Holes

We will first define a hole in a network rigorously using the language of algebraic topology. The nodes and edges of a network are the building blocks of topological space defined on the network. The algebraic topology extends this concept further to a simplicial complex, which considers higher order elements with more than three nodes such as triangles. Given a node set $v_i \in V$, an element with $(k+1)$ nodes is called $k-$simplex $\sigma_k = [v_1, \ldots, v_{k+1}]$. Node, edge and filled-in triangle are then denoted as σ_0, σ_1 and σ_2. Note that we call σ_2 as the filled-in triangle in the simplicial complex to distinguish the unfilled-in triangle consisting of three nodes (σ_0) in a network. The collection of simplexes is a simplicial complex. The example of simplicial complex is shown in Fig. 1 (a).

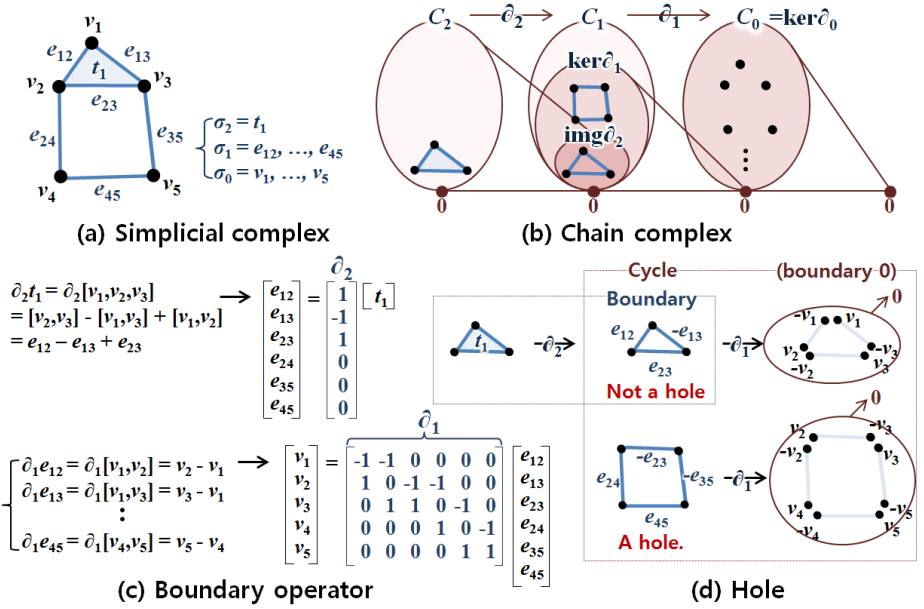

Fig. 1. (a) An example of simplicial complex. (b) A chain complex with chain, cycle and boundary groups which are mapped by boundary operator. (c) The boundary operators ∂_1 and ∂_2 of (a) in the matrix form. (d) A hole is the cycle whose boundary becomes zero, but not the boundary of any higher order simplex. Hence, the boundary of the filled-in triangle t_1 is not a hole but a cycle.

The boundary of an edge (σ_1) is two end nodes (σ_0) of the edge. The boundary of a filled-in triangle (σ_2) is three edges (σ_1) surrounding the triangle. If we denote C_k as a chain complex, a set of σ_ks, the relationship between σ_k and σ_{k-1} is defined using the boundary operator $\partial_k : C_k \to C_{k-1}$. Fig. 1 (b) shows a chain map by boundary operation. Given $\{\sigma_k^1, \cdots, \sigma_k^q\} \subset C_k$ and $\{\sigma_{k-1}^1, \cdots, \sigma_{k-1}^p\} \subset C_{k-1}$, the linear transformation $\partial_k \in \mathbb{R}^{p \times q}$ from C_k to C_{k-1} can be represented in the matrix form:

$$[\partial_k]_{ij} = \begin{cases} 1 \text{ if } \sigma_{k-1}^i \text{ is positively oriented w.r.t. } \sigma_k^j, \\ -1 \text{ if } \sigma_{k-1}^i \text{ is negatively oriented w.r.t. } \sigma_k^j, \\ 0 \text{ otherwise.} \end{cases}$$

When σ_{k-1}^i belongs to the ordered boundaries of σ_k^j, it is positively/negatively oriented if its order is odd/even. The matrix form of boundary operators is shown in Fig. 1 (c). ∂_1 is an incidence matrix of binary network. So the boundary operator is the generalization of the incident matrix in graph theory.

The kernel of ∂_k is a set defined by $\ker\partial_k = \{\sigma_k \in C_k | \partial_k \sigma_k = 0\}$. The kernel is then a cycle which consists of σ_ks starting and ending at the same σ_{k-1}. The image of ∂_{k+1} is a set defined by $\text{img}\partial_{k+1} = \{\sigma_k \in C_k | \partial_{k+1}\sigma_{k+1} = \sigma_k, \sigma_{k+1} \in C_{k+1}\}$. Hence, the image of ∂_{k+1} is a boundary of σ_{k+1}, which is always a cycle, i.e. $\text{img}\partial_{k+1} \subset \ker\partial_k$. But the cycle may not be a boundary of σ_{k+1} as shown in Fig. 1 (d), where the square hole is not the boundary of any higher order simplex. The set

of cycles of ∂_k, which are not the boundary of ∂_{k+1} is called the kth homology group. $H_k = \ker\partial_k \cap (\mathrm{img}\partial_{k+1})^C$, where $(\cdot)^C$ denotes the complementary set of $\cdot$ [7]. The element of H_k is the $k-$dimensional hole which is an important topological invariant used in distinguishing different topological spaces. The cardinality of H_k is the kth Betti number β_k. For the sake of simplicity, we will only consider 1-dimensional hole as a hole in this study and left higher dimensional holes as a future study.

2.2 $k-$Laplacian

In the persistent homology, the $k-$dimensional hole H_k is usually identified by manipulating the kernel of ∂_k and image of ∂_{k+1} based on Gaussian elimination [7]. If we apply this approach to the example in Fig. 1 (a), one of two possible holes, $e_{12}-e_{13}+e_{24}-e_{35}+e_{45}$ or $-e_{23}+e_{24}-e_{35}+e_{45}$, are estimated depending on how to order edges in the column of ∂_1 and row of ∂_2. To avoid this ambiguity, we introduce a new method based on $k-$Laplacian for estimating hole [10].

The k-Laplacian $\boldsymbol{L}_k$ is defined as $\boldsymbol{L}_k = \partial_{k+1}\partial_{k+1}^\top + \partial_k^\top\partial_k$ [11]. Since $\partial_0 : C_0 \to 0$, $\boldsymbol{L}_0 = \partial_1^\top\partial_1$ and it is the graph Laplacian, which is widely used in spectral clustering [12]. The kth homology group H_k is a kernel of $k-$Laplacian $\boldsymbol{L}_k$ [10]. Hence the kth Betti number β_k is the dimension of kernel space of $\boldsymbol{L}_k$. The eigenvectors with zero eigenvalues of $\boldsymbol{L}_k$ are spanned in the kernel space of $\boldsymbol{L}_k$. So, the $k-$dimensional hole in H_k is obtained by the eigenvectors with zero eigenvalues of $\boldsymbol{L}_k$. β_k is obtained by the number of zero eigenvalues of $\boldsymbol{L}_k$.

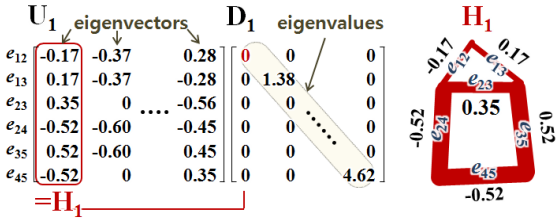

Fig. 2. Example of hole estimation based on eigenvector $\boldsymbol{U}_1$ and eigenvalue $\boldsymbol{D}_1$ of $\boldsymbol{L}_1$. The absolute value of eigenvector with zero eigenvalue becomes the edge weight in the hole H_1.

Fig. 2 shows the example of hole estimation using the spectrum of $\boldsymbol{L}_1$. The simplicial complex in Fig. 1 (a) is used as an example. After estimating $\boldsymbol{L}_1$ using ∂_1 and ∂_2 in Fig. 1 (c), we obtain its eigenvectors $\boldsymbol{U}_1$ and their corresponding eigenvalues $\boldsymbol{D}_1$. The eigenvector with zero eigenvalue of $\boldsymbol{L}_1$ is the hole H_1. The resulting hole can be represented in the linear combination of edges $-0.17e_{12} + 0.17e_{13} + 0.35e_{23} - 0.52e_{24} + 0.52e_{35} - 0.52e_{45}$ as shown in Fig. 2. The absolute value of coefficient is proportional to its contribution to the hole.

2.3 Persistent Holes

The metabolic brain connectivity forms the connectivity matrix $\boldsymbol{W} = [w_{ij}]$, with each of the elements w_{ij} encoding the distance between two brain regions v_i and v_j. We introduce the Rips complex to estimate holes in brain network with the connectivity matrix $\boldsymbol{W}$. The Rips complex $\mathcal{R}(\boldsymbol{W}, \epsilon)$ is a simplicial complex whose k-simplexes correspond to unordered $(k+1)$-tuples of nodes which are pairwise within distance ϵ [3]. If we confine $k \leq 1$, the Rips complex is identical

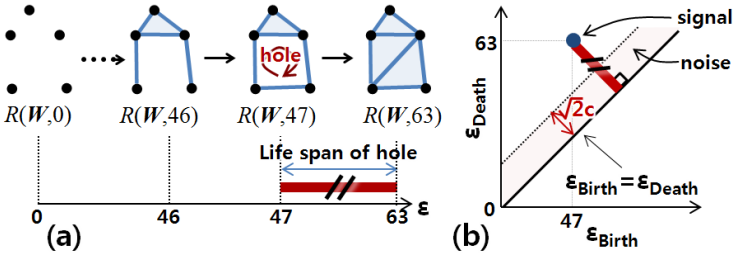

Fig. 3. (a) Rips filtration and (b) the persistence diagram of hole. Since the hole starts and ends at 47 and 63, respectively, the point is plotted at (47,63) on (b).

to the binary network where two nodes are connected if their distance is less than ϵ. Given the connectivity matrix $\boldsymbol{W}$ and thresholds $\epsilon_1 < \cdots < \epsilon_q$, the Rips filtration decomposes the connectivity matrix into the sequence of Rips complexes: $\mathcal{R}(\boldsymbol{W}, \epsilon_1) \subseteq \mathcal{R}(\boldsymbol{W}, \epsilon_2) \subseteq \cdots \subseteq \mathcal{R}(\boldsymbol{W}, \epsilon_q)$. During the filtration, the holes of Rips complexes are appearing and disappearing as shown in Fig. 3 (a). The persistent homology observes such a change of $k-$dimensional holes and counts their Betti numbers over the change of threshold. The birth and death times of hole ϵ_{Birth} and ϵ_{Death} are encoded in the persistence diagram by mapping to the point $(\epsilon_{Birth}, \epsilon_{Death})$. The persistence diagram $\mathcal{P}$ is a set of the points in the plane where the horizontal and vertical axes represent the birth and death times of hole as shown in Fig. 3 (b). The life span of hole from birth to death time is same as the distance from the point to the line $\epsilon_{Birth} = \epsilon_{Death}$ in the persistence diagram. The closer to the line $\epsilon_{Birth} = \epsilon_{Death}$, the shorter the life span of corresponding hole is. The persistent homology assumes that a persistent hole with long life span may be the signal that reflects the shape of true topological space, but a hole with short life span may be a noise. Now, we introduce the bottleneck distance to estimate the confidence band $[0, c]$ which distinguishes between signal and noise in Fig. 3 (b) [13].

The bottleneck distance W_∞ measures the distance between two persistence diagrams $\mathcal{P}_1$ and $\mathcal{P}_2$. It is defined as

$$W_\infty(\mathcal{P}_1, \mathcal{P}_2) = \min_P \max_{(x,y)\in P} d_\infty(x, y) \text{ for all } x \in \mathcal{P}_1, y \in \mathcal{P}_2,$$

where d_∞ is the L_∞ distance and P is a one-to-one correspondence of the points in $\mathcal{P}_1$ and $\mathcal{P}_2$. Suppose that the persistence diagrams of the underlying Rips and random Rips complexes $\mathcal{P}$ and $\mathcal{P}_{rand}$ are given. If we find a confidence interval c such that $P(W_\infty(\mathcal{P}, \mathcal{P}_{rand}) > c) \leq \alpha$, $\sqrt{2}c$ is same as the distance to the line $\epsilon_{Birth} = \epsilon_{Death}$ which distinguishes between the signal and noise [13]. The random Rips complexes are generated from 5000 random permutations of AD, MCI and NC datasets. For each permutation, the group labels are randomly reassigned and the persistence diagram $\mathcal{P}_{rand}$ and the bottleneck distance $T = W_\infty(\mathcal{P}, \mathcal{P}_{rand})$ are recalculated. After 5000 permutations, we obtain 5000 bottleneck distances and sort them in descending order as $T_1 > T_2 > \cdots > T_{5000}$. $c = T_{250}$ is chosen to satisfy $\alpha = 0.05$. Then, the hole located outside of the confidence band $[0, c]$ is denoted as the persistent hole. Here we expect that finding persistent holes may help understand aberrant functional connectivity in AD.

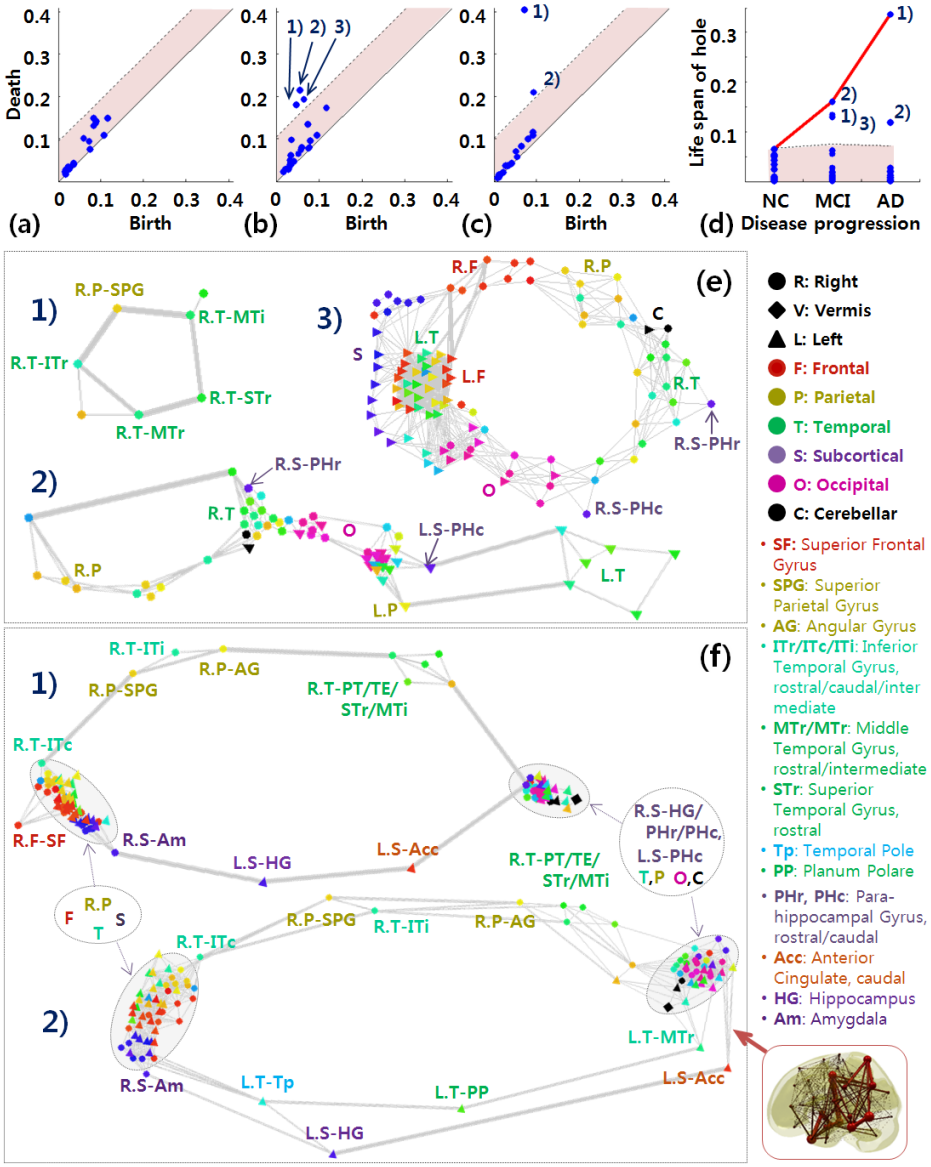

Fig. 4. The persistence diagram of (a) NC, (b) MCI and (c) AD. (d) The life span of hole with respect to the disease progression. There is no significantly persistent hole in NC. (e) Three persistent holes of MCI are mainly located in 1) right temporal, 2) bilateral temporo-parietal, and 3) widespread fronto-temporo-parietal-occipital lobule. (f) Two persistent holes of AD may occur because the limbic-temporo-parietal association regions disturb direct connections between two large clustered regions.

3 Results

Data Sets. We used FDG-PET imaging data sets: 45 NC (age: 68.9 ± 5.2), 24 MCI (67.8 ± 9.0) and 22 AD (66.9 ± 7.1) subjects. All ^{18}F-FDG PET images were spatially normalized and smoothed with 16 mm FWHM using the SPM package. Then, FDG uptake values of 103 regions of interest (ROIs) were extracted by weighted averaging. Each FDG uptake value was scaled by individual's total gray matter mean count. The connectivity matrix $\boldsymbol{W} = [w_{ij}] \in \mathbb{R}^{103\times 103}$ was estimated based on the diffusion distance on positive correlation between FDG uptake values in two ROIs.

Group Differences. The persistence diagrams of NC, MCI and AD are shown in Fig. 4 (a-c). The total number of holes is 17 for AD, 25 for MCI and 21 for NC. We examined group differences using the bottleneck distance between persistence diagrams and permutation test. The persistence diagrams are significantly different between NC and AD ($p < 0.05$), but tend to be different between NC and MCI and between MCI and AD ($p < 0.1$).

Life Span of Holes. In Fig. 4 (d), the life span of holes is plotted with respect to NC, MCI and AD. Using the permutation test, we found that the longest life span of holes connected by red line is proportional to the disease progression ($p < 0.05$). The resulting confidence band for persistence diagram is shown in the shaded region in Fig. 4 (a-d). All holes in NC are not persistent. 2 and 3 holes are determined as the persistent for AD and MCI respectively.

Persistent Hole. 5 persistent holes are shown in Fig. 4 (e,f). Three persistent holes of MCI are mainly located in right temporal, bilateral temporo-parietal, and widespread fronto-temporo-parietal-occipital lobule. The reduced metabolism in a network has been found in parietal, temporal and frontal lobes in AD [8]. Especially, the hypometabolism of medial temporal lobe observed in the first hole is known as a biomarker for the identification of MCI [9]. In the persistent holes of AD, we found that two large clustered brain regions on the left and right sides in (f) are not directly connected because the limbic-temporo-parietal association regions disturb the connection between them. These association regions are also known to be affected by AD [8,9].

4 Conclusions

In this study, we propose a new method for localizing aberrant regions by detecting hole in the metabolic network based on persistent homology and 1-Laplacian. We also introduce a new biomarker, life span of hole, to measure the degree of abnormality of brain network. The proposed hole detection method is natural extension of finding modular structure of network based on the spectrum of graph Laplacian, $0-$Laplacian. The resulting aberrant holes are mainly located in parietal, temporal and frontal regions which is known to be related to AD and MCI. In addition, our finding suggests that the brain network inefficiency in AD

may be because the limbic-temporo-parietal association regions interrupt direct connections between other brain regions. The proposed method can be further applicable to other high order topologically invariant features using k-Laplacian, which is left as a future study.

Acknowledgments. This work was supported by Basic Science Research Program through the National Research Foundation of Korea (NRF) funded by the Ministry of Education (2013R1A1A2064593), by NRF grant funded by the Korea government (MEST) (2011-0030815), by a grant of the future-based technology development programof the NRF funded by the MEST (20100028755) and by NIH grant UL1TR000427 and Vilas Associate Award from Univ. of Wisconsin.

References

1. Park, H., Friston, K.: Structural and functional brain networks: from connections to cognition. Science 342(6158), 1238411 (2013)
2. Carlsson, G.: Topology and data. B. Am. Math. Soc. 46, 255–308 (2009)
3. Lee, H., Chung, M.K., Kang, H., Kim, B.N., Lee, D.S.: Persistent brain network homology from the perspective of dendrogram. IEEE T. Med. Imaging 31, 2267–2277 (2012)
4. de Silva, V., Ghrist, R.: Coverage in sensor networks via persistent homology. Algebraic and Geometric Topology 7, 339–358 (2007)
5. Muhammad, A., Egerstedt, M.: Control using higher order laplacians in network topologies. In: Proceedings of the 17th International Symposium on Mathematical Theory of Networks and Systems, pp. 1024–1038 (2006)
6. Daianu, M., Jahanshad, N., Nir, T.M., Toga, A.W., Jack, C.R., Weiner, M.W., Thompson, P.M.: Breakdown of brain connectivity between normal aging and alzheimer's disease: A structural k-core network analysis. Brain Connectivity 3(4), 407–422 (2013)
7. Edelsbrunner, H., Harer, J.: Computational Topology: An Introduction. American Mathematical Society Press (2009)
8. Alexander, G.E., Chen, K., Pietrini, P., Rapoport, S.I., Reiman, E.M.: PET evaluation of cerebral metabolic decline in dementia: A potential outcome measure in alzheimer's disease treatment studies. Am. J. Psychiatry 159, 738–745 (2002)
9. Mosconi, L., Tsui, W.H., De Santi, S., Li, J., Rusinek, H., Convit, A., Li, Y., Boppana, M., de Leon, M.J.: Reduced hippocampal metabolism in MCI and AD: automated FDG-PET image analysis. Neurology 64, 1860–1867 (2005)
10. Horak, D., Jost, J.: Spectra of combinatorial laplace operators on simplicial complexes. Advances in Mathematics 244, 303–336 (2013)
11. Awasthi, V.V.: A note on the application of incidence matrices of simplicial complexes. Int. Journal of Contemp. Math. Sciences 8(19), 935–939 (2013)
12. Chung, F.R.K.: Spectral Graph Theory. CBMS Regional Conference Series in Mathematics, No. 92. American Mathematical Society (1996)
13. Balakrishnan, S., Fasy, B.T., Lecci, F., Rinaldo, A., Singh, A., Wasserman, L.: Statistical inference for persistent homology (2013)